JACS
JOURNAL OF THE AMERICAN CHEMICAL SOCIETY

ARTICLE

pubs.acs.org/JACS

Water (in Water) as an Intrinsically Efficient Proton Acceptor in Concerted Proton Electron Transfers

Julien Bonin, Cyrille Costentin, Cyril Louault, Marc Robert, and Jean-Michel Savéant*

Laboratoire d'Electrochimie Moléculaire, Unité Mixte de Recherche Université - CNRS No 7591, Université Paris Diderot, Bâtiment Lavoisier, 15 rue Jean de Baïf, 75205 Paris Cedex 13, France

Supporting Information

ABSTRACT: The oxidation of PhOH in water by photochemically generated $Ru^{III}(bpy)_3$ is taken as prototypal example disclosing the special character of water, in the solvent water, as proton acceptor in concerted proton−electron transfer reactions. The variation of the rate constant with temperature and driving force, as well as the variation of the H/D kinetic isotope effect with temperature, allowed the determination of the reaction mechanism characterized by three intrinsic parameters, the reorganization energy, a pre-exponential factor measuring the vibronic coupling of electronic states at equilibrium distance, and a distance-sensitivity parameter. Analysis of these characteristics and comparison with a standard base, hydrogen phosphate, revealed that electron transfer is concerted with a Grotthus-type proton translocation, leading to a charge delocalized over a cluster involving several water molecules. A mechanism is thus uncovered that may help in understanding how protons could be transported along water chains over large distances in concert with electron transfer in biological systems.

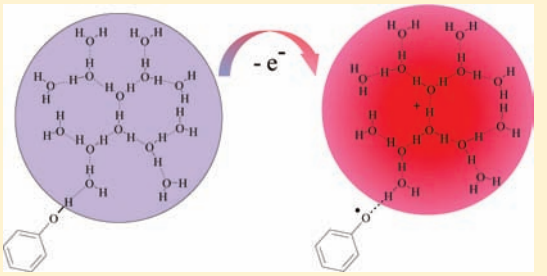

INTRODUCTION

Association between electron and proton transfers is omnipresent in natural and artificial systems and is expected to play a crucial role in the resolution of contemporary energy challenges. These proton-coupled electron transfers (PCET) may follow stepwise and/or concerted pathways[1−4] as illustrated in Figure 1 with the example of phenol oxidation. The concerted pathway (CPET) is of particular interest because it avoids passing through the high energy intermediates involved in the two stepwise pathways, PET (proton transfer followed by electron transfer) and EPT (electron transfer followed by proton transfer). Unraveling the mechanisms of proton-coupled electron transfers, where proton and electron transfers involve different molecular centers, is an important task in conjunction with the relevance of these reactions to a huge number of natural and artificial systems. Although the concerted-stepwise competition is a completely general issue, illustration by phenol oxidation in Figure 1 refers to the prominent role phenols play in reactions occurring in natural systems particularly, but not exclusively, to the oxidation of tyrosine in Photosystem II.[5−12] Phenols bearing an amine group so as to mimic the oxidation of tyrosine with transfer of the proton to a neighboring base have received a lot of attention including detailed analysis of the mechanisms and dynamics of the reaction.[13−18] Besides these examples, the role of water in PCET reactions where water is used as solvent is obviously of considerable interest with reference to both natural and artificial systems.

Concerning the latter, one has in mind the reductive or oxidative transformation of small molecules such as water, dioxygen, and carbon dioxide in an effort to address contemporary energy challenges.[19−21] It is also an important fundamental

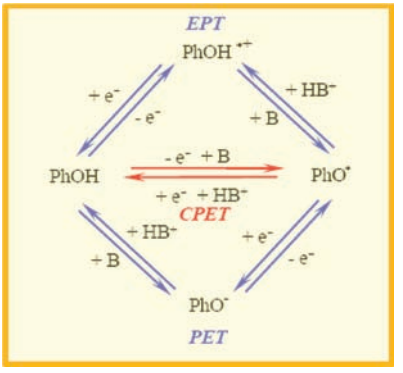

Figure 1. PCET stepwise (blue) and concerted (red) pathways.

issue. Indeed, although they have been investigated over decades, the structure of proton in water and mechanisms of proton conduction therein continue to be under active experimental and theoretical scrutiny.[22−26] Along the same lines, the mechanism of PCET reactions involving water as proton acceptor should deserve the same attention. Homogeneous[27−29] and electrochemical[30−33] oxidations of phenols with water as sole proton acceptor have been the object of several investigations. As seen in the following, these reactions may serve to uncover the intrinsic features of water as proton acceptor in CPET. The most recent work in this area has shown, based on rate

Received: December 6, 2010
Published: April 08, 2011

constant—driving force variations, that the reaction is characterized by very large intrinsic rate constants (rate constant at zero driving force).[27,33] However, what has been lacking so far is the gathering of data that would allow dissecting phenol oxidation reactivity to reveal the various intrinsic parameters characterizing CPET dynamics: reorganization energy, equilibrium pre-exponential factor picturing electronic states coupling, and distance-sensitivity parameter featuring the ability of proton to travel over large distances in water in concert with electron transfer. Such an analysis is indeed required to be au fait with what makes water a special proton acceptor in CPET reactions. This is the subject of the present article.

We first describe the variation with temperature of the rate constant for the reaction of the photogenerated $Ru^{III}(bpy)_3$ with phenol, leading to an Arrhenius plot that allows, after careful analysis, the separate derivation of the reorganization energy, of the equilibrium pre-exponential factor, and of the distance—sensitivity parameter. The photochemical technique we used consists of generating the Ru(III) complex by quenching of the photoexcited Ru(II) complex by the methylviologen dication (MV^{2+}).[27]

To uncover the reasons of the peculiar characteristics of water (in water) as the proton acceptor, a comparative analysis of the oxidation of phenol in the presence of a standard base, hydrogen phosphate, was carried out. In both cases, besides the recording of Arrhenius plots, determination of the H/D isotope effect and of its variation with temperature were essential pieces of data to elucidate mechanisms and kinetic parameters.

RESULTS

H_2O-CPET Oxidation of Phenol by $Ru^{III}(bpy)_3$. The variations with temperature of the pseudosecond-order rate constant of the reaction of $Ru^{III}(bpy)_3$ with phenol at three different pH's are summarized in Figure 2a.

The data points at pH's 2 and 4 are practically the same over the whole range of temperature, whereas there is a definite increase of the rate constant when going to pH = 7.2. This observation confirms and generalizes previous results obtained at 25 °C, pointing to the occurrence of H_2O-CPET at the first pH's and to an increased superposition of this pathway and of an OH^--PET pathway as the pH increases.[27]

Repeating the above pH 2 experiment in D_2O (Figure 2b) allows the determination of the H/D isotope effect characterizing the H_2O-CPET as a function of temperature (Figure 2c).

The observation of a substantial H/D isotope effect confirms the concerted character of the reaction. Its clear decrease with temperature will be a quite useful piece of information in the foregoing discussion of the special character of water as the proton acceptor.

The straight lines in Figure 2b therefore represent the Arrhenius plots for the CPET reaction in H_2O and D_2O, respectively:

$$\ln k_{H_2O} = 24.70(\pm 0.05) - \frac{3175(\pm 15)}{T} \quad (1)$$

$$\ln k_{D_2O} = 26.10(\pm 0.05) - \frac{4020(\pm 15)}{T} \quad (2)$$

For the estimation of uncertainties, see the Supporting Information.

PO_4H^{2-}-CPET Oxidation of Phenol by $Ru^{III}(bpy)_3$. The variation with temperature of the pseudosecond-order rate constant of the reaction of $Ru^{III}(bpy)_3$ with phenol in a phosphate buffer at pH = 7.2, k^H_{buf}, is summarized in Figure 3a,b. The

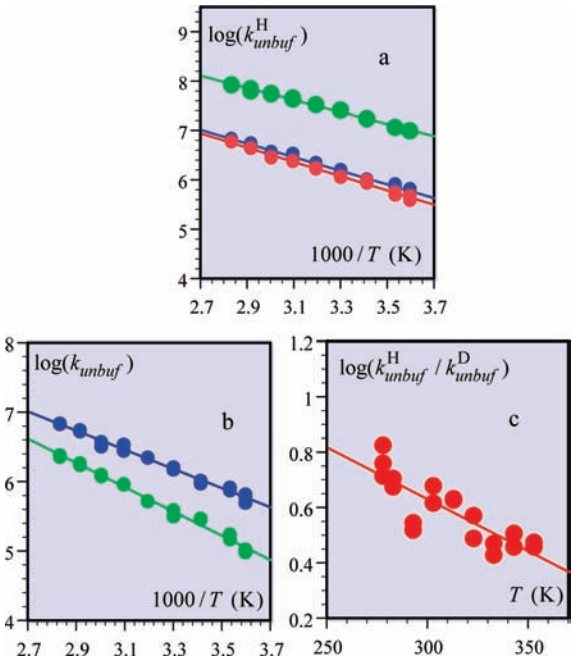

Figure 2. (a) Pseudosecond-order rate constant (in M^{-1} s^{-1}) of the reaction of $Ru^{III}(bpy)_3$ with phenol in unbuffered media at pH = 2 (blue dots), 4 (red dots), and 7.2 (green dots) as a function of temperature. (b) Variation of the pseudosecond-order rate constant (in M^{-1} s^{-1}) with temperature in H_2O (blue dots) and D_2O (green dots) at pH = 2. (c) Variation of the H/D isotope effect ($=k^H_{unbuf}/k^D_{unbuf}$) with temperature.

value of k^H_{buf} results from the superimposition of three pathways, H_2O-CPET, OH^--PET, and PO_4H^{2-}-CPET:

$$k^H_{buf} = k^{CPET,H}_{H_2O} + k^{PET,H}_{OH^-} + k^{CPET,H}_{PO_4H^{2-}}[PO_4H^{2-}]$$
$$= k^H_{unbuf,pH=7.2} + k^{CPET,H}_{PO_4H^{2-}}[PO_4H^{2-}] \quad (3)$$

This is the reason that our results are not easy to compare with previous results concerning the oxidation of a closely resembling phenol, tyrosine, in the presence of hydrogen phosphate where the H_2O-CPET pathway was not taken into account.[34,35]

Figure 3c shows the application of eq 3 to the data in Figure 3a and b leading to the extraction of the third-order rate constant $k^{CPET,H}_{PO_4H^{2-}}$ as a function of temperature. The data points corresponding to the three hydrogen phosphate concentrations fall on the same Arrhenius line (Figure 3c). This proportionality of the rate to the hydrogen phosphate concentration justifies the assumption made above that the reaction follows a CPET pathway rather than a stepwise pathway, PET or EPT, for the following reasons. Concerning the PET pathway, the driving force for the deprotonation step is $10^{-(pK_{PhOH}-pK_{PO_4H_2^-})} = 10^{-2.8}$ in terms of equilibrium constant at 25 °C and very close to this value at the other temperatures. The reprotonation reaction is thus expected to be at the diffusion limit, as is the follow-up oxidation of the phenoxide ion by $Ru^{III}(bpy)_3$.[32] Because hydrogen phosphate concentration is much larger than the $Ru^{III}(bpy)_3$ concentration, the deprotonation step is a pre-equilibrium step preceding the rate-determining electron transfer to phenoxide ion. In these conditions, the rate constant is predicted to be independent of the hydrogen phosphate concentration at the fixed pH of 7.2 in contrast with the experimental data, thus ruling out the occurrence of the PET pathway. In the EPT case, the

dx.doi.org/10.1021/ja110935c | J. Am. Chem. Soc. 2011, 133, 6668–6674

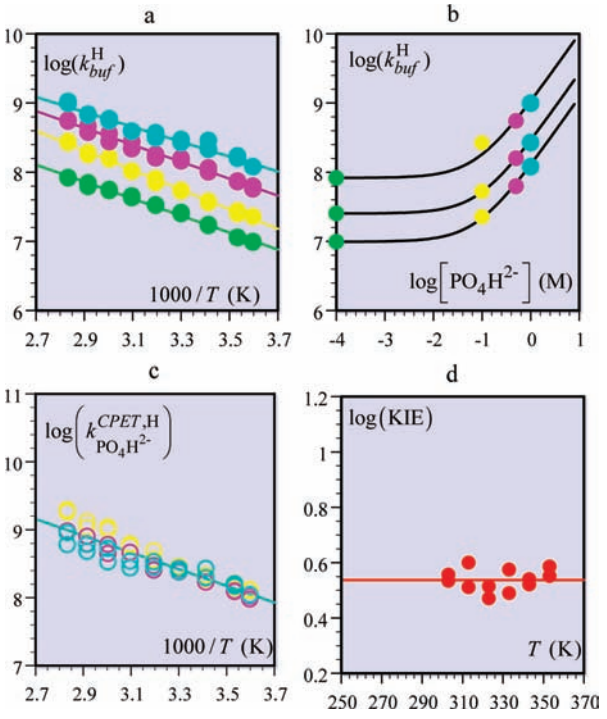

Figure 3. Reaction of $Ru^{III}(bpy)_3$ with phenol in phosphate buffered medium at pH = 7.2 for a total concentration of phosphate of 0 (green), 0.1 (yellow), 0.5 (magenta), and 1 M (cyan). (a) Variation of the global pseudosecond-order rate constant (in M^{-1} s^{-1}) with temperature. (b) Variation of the global pseudosecond-order rate constant (in M^{-1} s^{-1}) with $[PO_4H^{2-}]$ at, from bottom to top, 278, 303, and 353 K. (c) Extraction of the third-order rate constant (in M^{-2} s^{-1}) for the reaction with hydrogen phosphate according to eq 3. Data in green correspond to average values. (d) H/D isotope effect as a function of temperature.

follow-up deprotonation is an extremely downhill reaction (a driving force of $10^{-(pK_{PhOH^{\bullet+}}-pK_{PO_4H_2^-})} = 10^{9.2}$ in terms of equilibrium constant at 25 °C), making the electron transfer from PhOH to $Ru^{III}(bpy)_3$ the rate-determining step. The reaction rate is therefore predicted to be independent of the hydrogen phosphate concentration at the fixed pH of 7.2, unlike the experimental observations, thus ruling out the occurrence of the EPT pathway. The variation of the third-order rate constant $k^{CPET,D}_{PO_4H_2^-}$ with temperature for the reaction with hydrogen phosphate in D_2O was derived from the values of k^{D}_{unbuf} (Figure 2b) by means of eq 3 leading to an H/D isotope effect shown in Figure 3d. The prevalence of the $PO_4H_2^-$-CPET pathway over the PET and EPT pathways is thus confirmed by these data, which indicate an H/D isotope effect of 3.5. It is remarkable that the H/D isotope effect does not vary with temperature (Figure 3d) unlike the case of water (Figure 2c). This observation will be quite useful in the foregoing discussion of the compared kinetics of water and hydrogen phosphate as proton acceptors in the oxidation of phenol by $Ru^{III}(bpy)_3$.

Summarizing the Arrhenius data for the hydrogen phosphate:

$$\ln k_{H_2O} = 28.70(\pm 0.05) - \frac{2830(\pm 15)}{T} \quad (4)$$

$$\ln k_{D_2O} = 30.70(\pm 0.05) - \frac{3420(\pm 15)}{T} \quad (5)$$

For the estimation of uncertainties, see the Supporting Information.

DISCUSSION

The following analysis of the results reported in the preceding section is based on a model whose main features, summarized in Figure 4, derive from a double application of the Born−Oppenheimer approximation. The transition state is located at the crossing of the potential energy profiles of the reactant and product systems toward the heavy-atom coordinate (parabola in Figure 4). We may therefore start from the following Marcus-type expression of the rate constant:[4,17,36,37]

$$k = Z \exp\left[-\frac{w_R}{RT}\right] \exp\left[-\frac{\lambda}{4RT}\left(1 + \frac{\Delta G^0 - w_R + w_P}{\lambda}\right)^2\right] \quad (6)$$

The pre-exponential factor, Z, is obtained from the termolecular pre-exponential factor, Z_{ter}, as $Z = Z_{ter}[B]$, where, in the case of water, $[B] = 1$ M is the activity of water in water and Z_{ter} is the pre-exponential factor of the reverse reaction, $PhO^{\bullet} + Ru^{II} + H^+$. In the case of hydrogen phosphate, $[B] = 1$ M and Z_{ter} is the pre-exponential factor of the direct reaction as well as the reverse reaction. Z_{ter} is a combined measure of the formation of precursor complexes over a range of significant reacting distances, on one hand, and of the efficiency of proton tunneling through the barrier shown in the upper inset of Figure 4, on the

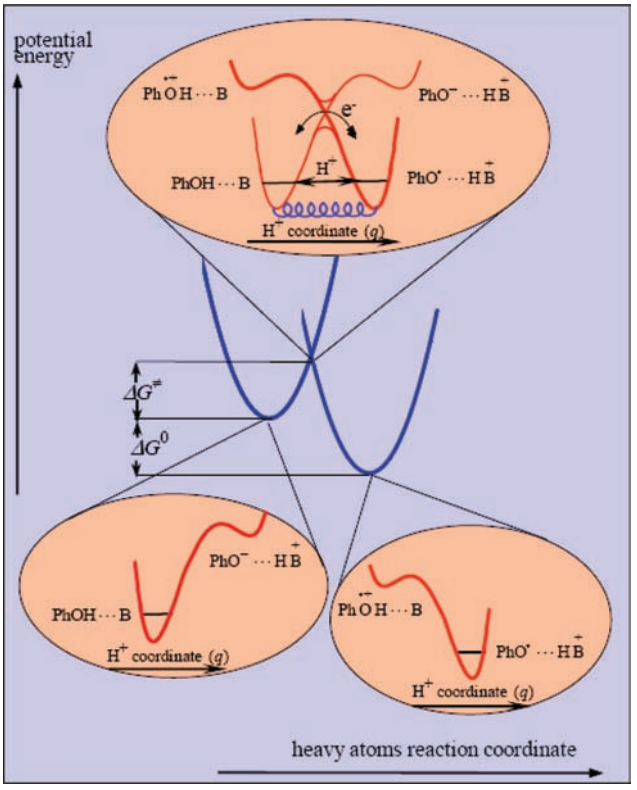

Figure 4. Potential energy curves for the reorganization of the heavy atoms of the system, including solvent molecules (parabola), and for the proton displacement concerted with electron transfer (upper insets). The symbols are defined in Figure 1 and in the text.

dx.doi.org/10.1021/ja110935c | J. Am. Chem. Soc. 2011, 133, 6668–6674

other hand. As developed in the Supporting Information, it may be expressed by eq 7:[38]

$$Z_{ter} = Z_{eq} \exp\left(\frac{2RT\beta^2}{f}\right) \quad (7)$$

which involves the combination of two intrinsic parameters: an equilibrium pre-exponential factor Z_{eq} (see Supporting Information for the derivation of the expression of Z_{eq}), characterizing the coupling of electronic states in the transition state at equilibrium distance (Figure 5), and a distance−sensitivity parameter β^2/f in which β is the attenuation factor of the exponential decay of the vibronic coupling of the two states with distance and f is the force constant of the harmonic oscillator of the H-bond between PhOH and the proton acceptor B.

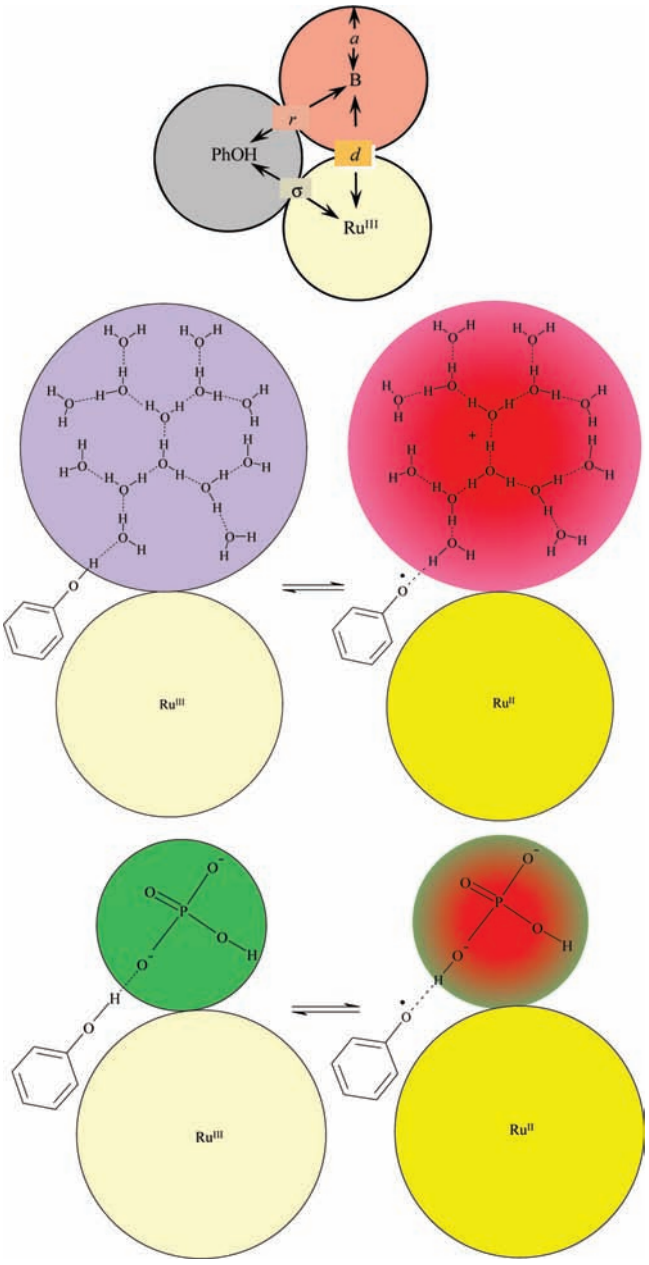

Figure 5. Third-order reacting clusters.

In the Franck−Condon exponential term of eq 6, λ is the reorganization energy, ΔG^0 is the reaction standard free energy, and w_R and w_P are the electrostatic work terms required to bring the reactants and products, respectively, from infinite separation to reacting distance.

When comparing several proton acceptors, as we do here with water and hydrogen phosphate, the driving force characteristics should be carefully separated from the intrinsic characteristics. For example, here, hydrogen phosphate has a driving force advantage of 7.2 pH units at 25 °C. We are in fact interested by comparing intrinsic characteristics, which may be in favor of water even though phosphate is more efficient in terms of driving force. Thus, we are looking for the comparison of the rate constants at zero driving force, with the additional ambition of dissecting this intrinsic rate constant into pre-exponential factor and reorganization energy. Albeit small, thermodynamic effects have also been taken into account when comparing the rate constants in H_2O and D_2O (see the Supporting Information).

Arrhenius plots such as those in Figures 2b and 3c, obtained by linearization of eq 6 in the nonadiabatic limit around the middle of the temperature range, T_m (313 K in our case), lead to expressions of the Arrhenius intercept and slope that contain three terms (see the linearization details and the ensuing expressions of the intercept and slope in the Supporting Information): one related to an intrinsic parameter, one related to a thermodynamical effect, and one related to a distance−sensitivity parameter. The three intrinsic parameters, λ, Z_{eq}, and β^2/f, were therefore obtained as follows. In the case of water, the slope and the intercept of the Arrhenius plot (Figure 2b) provide two relationships between these three parameters. A third relationship is obtained from the variations of the rate constant with the driving force using the data reported in ref 27. The resulting values of the three parameters are reported in Table 1. All ingredients required for the full analysis of the reaction kinetics that led to the determination of these three parameters are gathered together in the Supporting Information.

A first interesting observation is that the reorganization energy in the case of water as proton acceptor is much smaller than in the case of hydrogen phosphate, see later for the determination of parameters in the case of hydrogen phosphate. Because the difference between the two cases relates essentially to solvent reorganization, it may be concluded that the volume over which the positive charge is delocalized is larger in the first case than in the second, implying that, in the case of water, the positive charge does not involve a single water molecule. A more quantitative, although approximate, picture of solvent reorganization upon proton release during phenol oxidation may be obtained as follows. A first step consists of separating what concerns the CPET oxidation of phenol from what concerns the corresponding reduction of the oxidant partner, $Ru^{III}(bpy)_3$, according to:

$$\lambda = \frac{\lambda_{ox} + \lambda_{CPET}}{2} \quad (8)$$

where the overall reorganization energy, λ, is split into two contributions, λ_{ox}, relative to $Ru^{III}(bpy)_3$ self-exchange:

$$Ru^{II} + Ru^{III} \rightleftarrows Ru^{III} + Ru^{II}$$

and λ_{CPET} relative to the CPET self-exchange:

$$(PhOH\cdots B) + (PhO^{\bullet}\cdots {}^{+}HB) \rightleftarrows (PhO^{\bullet}\cdots {}^{+}HB) + (PhOH\cdots B)$$

dx.doi.org/10.1021/ja110935c | J. Am. Chem. Soc. 2011, 133, 6668–6674

Table 1. Kinetics Parameters of the H_2O-CPET and PO_4H^{2-}-CPET Oxidation of Phenol[a]

parameters	H_2O	PO_4H^{2-}
λ (=$(\lambda_{ox}+\lambda_{CPET})/2$)[b]	0.51 ± 0.02	0.72 ± 0.02
λ_{CPET} (eV)	0.45 ± 0.04	0.86 ± 0.04
$2R(\beta^2)/f$ (K^{-1})	0.0125 (H) 0.020 (D) ± 0.001	0 (H) 0.0064 (D) ± 0.001
$\ln Z_{eq} = \ln\left\{[4\pi N_A\sigma^2\sqrt{\langle\delta\sigma^2\rangle}\sqrt{\pi/2}] \times \left[4\pi N_A r^2\sqrt{\frac{RT}{f}}\sqrt{\pi/2}\right] \times \left[\frac{2}{\sqrt{\lambda}}\left(\frac{\pi}{RT}\right)^{3/2} C_{eq}^2\right]\nu_n\right\}^c$	19.5 (H) ± 0.6 15.9 (D) ± 0.6	16.8 (H) ± 0.6 14.8 (D) ± 0.6

[a] For the estimation of uncertainties, see the Supporting Information. [b] λ_{ox} = 0.57 eV: self-exchange reorganization energy for the $Ru^{III/II}$ couple.[39] [c] For the definition of σ and r, see Figure 5. $(\langle\delta\sigma^2\rangle)^{1/2}$, amplitude of the variation of σ; f, force constant of the harmonic oscillator of the H-bond between PhOH and B; C_{eq}, coupling constant between the two electronic states in the transition state at equilibrium distance between PhOH and B; ν_n, nuclear frequency. β is the attenuation factor of the exponential decay of the vibronic coupling of the two states with distance.

The major part of this reorganization energy may be ascribed to solvent reorganization accompanying the generation of a water-solvated proton. It is noteworthy that the ensuing value of the reorganization energy, 0.45 eV, is remarkably small, much smaller than the value found for hydrogen phosphate (see below). The proton charge is accordingly not concentrated on a single hydrogen or even on a single protonated water molecule. To estimate the corresponding solvation radius, and hence the number of water molecules involved in the solvation cluster that is reorganized upon CPET, one may attempt to use the Marcus relationship:[40]

$$\lambda_{CPET} \approx \lambda_0 = \frac{e^2}{4\pi\varepsilon_0}\left(\frac{1}{\varepsilon_{op}}-\frac{1}{\varepsilon_S}\right)\frac{1}{2a} \qquad (9)$$

where a is the radius defined in Figure 5, and ε_{op} and ε_s are the optical and static dielectric constants. As discussed earlier in the equivalent electrochemical case, eq 9 overestimates the solvent reorganization energy, presumably because the Born model itself overestimates solvation free energies. On the basis of experimental observations concerning the electrochemical reduction of aromatic hydrocarbons in dimethylformamide,[41] eq 10 was proposed[42] to replace eq 9:

$$\lambda_0\ (\text{eV}) \cong \frac{3}{a\ (\text{Å})} \qquad (10)$$

We may use this equation to get a rough estimate of the radius of the water cluster, 6.5 Å, involved in solvent reorganization (Figure 5), compatible with recent spectroscopic observations.[43] It is also in agreement with the conclusions of a current study of the reduction of dioxygen in concentrated acid solutions where the proton plays the converse role of a reactant.[44] The proton acceptor is therefore not a single water molecule but a cluster containing many water molecules, indicating that the CPET process involves the concerted, although not necessarily synchronous, displacement of several protons in agreement with recent findings concerning photochemically triggered proton transfer.[45] If proton displacements were occurring sequentially, the first of these would involve strong localization of the proton charge inconsistently with the small value of the reorganization energy found experimentally. It should be, however, emphasized that the above estimate of the size of the water cluster is very approximate because eq 10 was derived for simple outersphere electron transfers, not for CPET reactions, and for a polar solvent, dimethylformamide, in which H-bonding is not involved as it is in the present case. The above size estimate is thus intended to provide not more than an order of magnitude.

Analysis of the H_2O-CPET kinetics is also helped by observing the variation of the H/D isotope effect with temperature (Figure 2c). The entropic terms are identical in H_2O and D_2O (see the Supporting Information), and we assume that the reorganization energy is also the same in both media, thus leading to the following expression of the isotope effect:

$$\ln\left(\frac{k_H}{k_D}\right) = \left\{\begin{array}{c}\left[\ln\left(\frac{Z_{eq,H}}{Z_{eq,D}}\right)+\frac{\Delta S^0-\Delta S_{W_R}+\Delta S_{W_P}}{2R}\left(\frac{\Delta H_H^0-\Delta H_D^0}{\lambda}\right)\right] \\ -\frac{1}{RT_m}\left(\frac{\Delta H_H^0-\Delta H_D^0}{\lambda}\right)\left(\lambda+\frac{\Delta H_H^0+\Delta H_D^0}{2}\right)\end{array}\right\} + T\left\{\frac{1}{2RT_m^2}\left(\frac{\Delta H_H^0-\Delta H_D^0}{\lambda}\right)\left(\lambda+\frac{\Delta H_H^0+\Delta H_D^0}{2}\right) + 2R\frac{(\beta_H^2-\beta_D^2)}{f}\right\} \qquad (11)$$

Therefore, taking the enthalpic terms ΔH_H^0 and ΔH_D^0 into account, the fitting of the linear variation of the isotope effect with temperature allows the determination of both intrinsic parameters, $2R(\beta_D^2)/f$ = 0.02 K^{-1} and ln $Z_{eq,D}$ = 15.9 in D_2O. Most of the isotope effect is due to intrinsic variations, the variation of the enthalpic term of the driving force upon changing hydrogen into deuterium being modest. As expected, the equilibrium pre-exponential factor Z_{eq}, characterizing the coupling of electronic states in the transition state at equilibrium distance, is smaller with deuterium than with hydrogen, and the distance–sensitivity parameter β^2/f is larger with deuterium than with hydrogen. These values are also compatible with the occurrence of a Grotthus-type mechanism during the CPET process. Additional evidence is provided by comparison with hydrogen phosphate.

In the latter case, Arrhenius plots can only be fitted by means of vanishingly small values of β^2/f. λ_{CPET} is then predicted (eq 8) to be equal to 0.86 eV for H and closely the same for D corresponding to a solvation radius of the order of 3.5 Å (Figure 5), corresponding to the value that can be derived from a volume using the Gaussian program to hydrogen phosphate (3.65 Å).[46]

In other words, the behavior of hydrogen phosphate as proton acceptor appears to be intrinsically different from that of water. The fact that the parameter β^2/f is vanishingly small may be interpreted as being due to a much stiffer phenol-base system and, in this sense, a less efficient CPET because the proton does

dx.doi.org/10.1021/ja110935c | J. Am. Chem. Soc. 2011, 133, 6668–6674

not travel over a large distance in concert with electron transfer. Accordingly, unlike the case of water, the H/D isotope effect does not depend significantly upon temperature.

We finally note that the third intrinsic parameter, the equilibrium pre-exponential factor, Z_{eq}, featuring the electronic states coupling from the precursor complex at its equilibrium distance, is larger in the case of water (3×10^8 M^{-2} s^{-1}) than in the case of hydrogen phosphate (2×10^7 M^{-2} s^{-1}), indicating that proton translocation is more efficient in water than it is for a conventional CPET process where the proton is more localized, in line with the conclusions drawn from the comparison between the solvent reorganization energies. Accordingly, the H/D isotope effect on Z_{eq} is larger in the case of water than in the case of hydrogen phosphate.

CONCLUSIONS

The oxidation of PhOH in unbuffered water by photochemically generated $Ru^{III}(bpy)_3$ has been taken as prototypal example of the special character of water, in the solvent water, as proton acceptor in a concerted proton−electron transfer (CPET) reactions. Three characteristic parameters could be derived from the temperature and driving force dependence of the rate constant, the solvent reorganization energy, the nonadiabatic pre-exponential factor at equilibrium distance of the proton donor and acceptor in the transition state, and the rate at which the coupling between the two vibronic states at the transition state varies with distance. Comparison with the same parameters derived in the case where hydrogen phosphate is the proton acceptor has been enlightening for unraveling what makes water, in water, a peculiar proton acceptor.

The relatively small value of the solvent reorganization energy, smaller than the value for the hydrogen phosphate, indicates that the charge of the proton produced upon phenol oxidation is delocalized over a large cluster of water molecules in line with recent spectroscopic findings.

In the case of water, the pre-exponential factor at equilibrium distance of the proton donor and acceptor in the transition state is 15 times larger than the same parameter for hydrogen phosphate, indicating an intrinsically very efficient concerted Grotthus-type H-bond relay proton displacement within the water cluster (Figure 5). The mechanism thus uncovered, involving a charge delocalization of the proton generated by oxidation over a large water cluster and the accompanying concerted Grotthus-type translocation of protons, may help in understanding how protons could be transported along water chains over large distances in concert with electron transfer in biological systems.

EXPERIMENTAL SECTION

Chemicals. Ultrapure water (18.2 MΩ cm) from a Milli-Q (Millipore) purification system or deuterium oxide (Euriso-Top, 99.9%) was employed to prepare the samples. $Ru(bpy)_3Cl_2 \cdot 6H_2O$ (Fluka, Technical grade), phenol (Fluka, Ultra, ≥99.5%), $HNa_2O_4P \cdot 12H_2O$ (Fluka, ≥99%), and $H_2NaO_4P \cdot 2H_2O$ (Acros, ≥99%) were used without further purification. Methylviologen dichloride hydrate (Aldrich, 98%) was recrystallized from ethanol and dried overnight in a vacuum before use.

Laser Flash Photolysis. The experimental setup for the flash-quench technique was the same as previously described.[27] Transient absorption measurements were conducted with a laser flash photolysis spectrometer (Edinburgh Instruments, LP920-KS). The solutions were excited at 460 nm (5 ns pulse, 6−8 mJ cm^{-2}) via an OPO (Continuum, SLOPO Plus) pumped by a frequency-tripled Nd:YAG laser (Continuum, Surelite II-10). Perpendicular analyzing light was provided by a 450 W ozone-free pulsed xenon lamp (Osram XBO) and was collected into a spectrograph. Kinetics at 450 nm for Ru^{2+}/Ru^{2+*} and at 605 nm for $MV^{\bullet+}$ were then measured thanks to a photomultiplier tube (Hamamatsu, R928) linked to a 100 MHz oscilloscope (Tektronix, TDS 3012C). Samples typically contained 50 μM of Ru complex, 40 mM of MV^{2+}, and 25 mM of phenol. Precise temperature of the sample port was set by a Peltier effect controller (Quantum Northwest TC125). The control and the synchronization of the whole setup were ensured by the Edinburgh Instruments L900 software. The sample pH was adjusted at room temperature with microvolumes of molar acid (HCl) or base (NaOH) and was controlled by a pH-meter (Hanna, pH 210) equipped with a microelectrode (6 mm, Bioblock Scientific). Change of the sample pH with temperature was independently measured and found to be negligible over the range studied. pK_a change upon temperature variation and deuteration was taken into account.[47−49] All samples were purged with argon for 15 min prior to the measurement.

Cyclic Voltammetry. Cyclic voltammetry was used to investigate the thermodynamics of the reaction (see the Supporting Information). It was performed with a standard three-electrode water-jacketed cell and an Autolab potentiostat (PGSTAT 12, Autolab) interfaced to a PC computed and driven with the GPES software (version 4.7). A saturated calomel electrode, isolated from the solution by a glass frit, and a platinum wire were used as reference and counter electrodes, respectively. Working electrode was a glassy carbon electrode (3 mm diameter) polished by a 3 and 1 mm alumina slurry on a cloth polishing pad and washed with water and ethanol under sonication. CVs were systematically recorded under argon pressure at each temperature.

ASSOCIATED CONTENT

Supporting Information. Further details accompany this Article and include theoretical analysis of the CPET kinetics, thermodynamics of the oxidation of phenol by $Ru^{III}(bpy)_3$, variations of the work terms with temperature, ensuing entropic, and enthalpic factors, and complete ref 46. This material is available free of charge via the Internet at http://pubs.acs.org.

AUTHOR INFORMATION

Corresponding Author
saveant@univ-paris-diderot.fr

ACKNOWLEDGMENT

Partial financial support from the Agence Nationale de la Recherche (Programme Blanc PROTOCOLE) is gratefully acknowledged.

REFERENCES

(1) Huynh, M. H. V.; Meyer, T. J. *Chem. Rev.* **2007**, *107*, 5004–5064.
(2) Costentin, C. *Chem. Rev.* **2008**, *108*, 2145–2179.
(3) Reece, S. Y.; Nocera, D. G. *Annu. Rev. Biochem.* **2009**, *78*, 673–699.
(4) Costentin, C.; Robert, M.; Savéant, J. M. *Acc. Chem. Res.* **2010**, *43*, 1019–1029.
(5) Stubbe, J.; van der Donk, W. A. *Chem. Rev.* **1998**, *98*, 705–762.
(6) Giese, B.; Wessely, S. *Chem. Commun.* **2001**, 2108–2109.
(7) Stubbe, J. *Chem. Commun.* **2003**, *2003*, 2511–2513.
(8) Byrdin, M.; Sartor, V.; Eker, A. P. M.; Vos, M. H.; Aubert, C.; Brettel, K.; Mathis, P. *Biochim. Biophys. Acta, Bioenerg.* **2004**, *1655*, 64–70.
(9) Rutherford, A. W.; Boussac, A. *Science* **2004**, *303*, 1782–1784.

(10) Meyer, T. J.; Huynh, M. H. V.; Thorp, H. H. *Angew. Chem., Int. Ed.* **2007**, *46*, 5284–5304.
(11) Shih, C.; Museth, A. K.; Abrahamsson, M.; Blanco-Rodriguez, A. M.; Di Bilio, A. J.; Sudhamsu, J.; Crane, B. R.; Ronayne, K. L.; Towrie, M.; Vlcek, A.; Richards, J. H.; Winkler, J. R.; Gray, H. B. *Science* **2008**, *320*, 1760–1762.
(12) Dempsey, J. L.; Winkler, J. R.; Gray, H. B. *Chem. Rev.* **2010**, *110*, 7024–7039.
(13) Maki, T.; Araki, Y.; Ishida, Y.; Onomura, O.; Matsumura, Y. *J. Am. Chem. Soc.* **2001**, *123*, 3371–3372.
(14) Rhile, I. J.; Mayer, J. M. *J. Am. Chem. Soc.* **2004**, *126*, 12718–9.
(15) Costentin, C.; Robert, M.; Savéant, J.-M. *J. Am. Chem. Soc.* **2006**, *128*, 4552–4553.
(16) Rhile, I. J.; Markle, T. F.; Nagao, H.; DiPasquale, A. G.; Lam, O. P.; Lockwood, M. A.; Rotter, K.; Mayer, J. M. *J. Am. Chem. Soc.* **2006**, *128*, 6075–6088.
(17) Costentin, C.; Robert, M.; Savéant, J. M. *J. Am. Chem. Soc.* **2007**, *129*, 9953–9963.
(18) Costentin, C.; Robert, M.; Savéant, J.-M. *Phys. Chem. Chem. Phys.* **2010**, *12*, 13061–13069.
(19) Savéant, J.-M. *Elements of Molecular and Biomolecular Electrochemistry: An Electrochemical Approach to Electron Transfer Chemistry*; John Wiley & Sons: Hoboken, NJ, 2006.
(20) *Acc. Chem. Res.* **2009**, *42*, 1859−2029.
(21) Nocera, D. G. *Inorg. Chem.* **2009**, *48*, 10001–10017.
(22) Laage, D.; Hynes, J. T. *Science* **2006**, *311*, 832–835.
(23) Marx, D. *ChemPhysChem* **2006**, *7*, 1848–1870.
(24) Hynes, J. T. *Nature* **2007**, *446*, 270–273.
(25) Paesani, F.; Voth, G. A. *J. Phys. Chem. B* **2009**, *113*, 5702–5719.
(26) Roberts, S. T.; Ramasesha, K.; Tokmakoff, A. *Acc. Chem. Res.* **2009**, *42*, 1239–1249.
(27) Bonin, J.; Costentin, C.; Louault, C.; Robert, M.; Routier, M.; Savéant, J.-M. *Proc. Natl. Acad. Sci. U.S.A.* **2010**, *107*, 3367–3375.
(28) Irebo, T.; Reece, S. Y.; Sjödin, M.; Nocera, D. G.; Hammarström, L. *J. Am. Chem. Soc.* **2007**, *129*, 15462–15464.
(29) Song, N.; Stanbury, D. M. *Inorg. Chem.* **2008**, *47*, 11458–11460.
(30) Richards, J. A.; Whitson, P. E.; Evans, D. H. *J. Electroanal. Chem.* **1975**, *63*, 311–327.
(31) Speiser, B.; Rieker, A. *J. Electroanal. Chem.* **1979**, *102*, 373–395.
(32) Costentin, C.; Louault, C.; Robert, M.; Savéant, J.-M. *J. Am. Chem. Soc.* **2008**, *130*, 15817–15819.
(33) Costentin, C.; Louault, C.; Robert, M.; Savéant, J.-M. *Proc. Natl. Acad. Sci. U.S.A.* **2009**, *106*, 18143–18148.
(34) Fecenko, C. J.; Meyer, T. J.; Thorp, H. H. *J. Am. Chem. Soc.* **2006**, *128*, 11020–11021.
(35) Fecenko, C. J.; Thorp, H. H.; Meyer, T. J. *J. Am. Chem. Soc.* **2007**, *129*, 15098–15099.
(36) Edwards, S. J.; Soudackov, A. V.; Hammes-Schiffer, S. *J. Phys. Chem. A* **2009**, *113*, 2117–2126.
(37) Hammes-Schiffer, S. *Acc. Chem. Res.* **2009**, *42*, 1881–1889.
(38) Soudackov, A. V.; Hatcher, E.; Hammes-Schiffer, S. *J. Chem. Phys.* **2005**, *122*, 014505–13.
(39) Sutin, N.; Brunschwig, B. S. *ACS Symp. Ser.* **1982**, *198*, 105–35.
(40) Marcus, R. A. *J. Chem. Phys.* **1965**, *43*, 679–701.
(41) Kojima, H.; Bard, A. J. *J. Am. Chem. Soc.* **1975**, *97*, 6317–6324.
(42) Savéant, J.-M. *Elements of Molecular and Biomolecular Electrochemistry: An Electrochemical Approach to Electron Transfer Chemistry*; John Wiley & Sons: Hoboken, NJ, 2006; p 60.
(43) Stoyanov, E. S.; Stoyanova, I. V.; Reed, C. A. *J. Am. Chem. Soc.* **2010**, *132*, 1484–5.
(44) Snir, O.; Wang, Y.; Tuckerman, M. E.; Geletii, Y. V.; Weinstock, I. A. *J. Am. Chem. Soc.* **2010**, *132*, 11678–11691.
(45) Cox, M. J.; Timmer, R. L. A.; Bakker, H. J.; Park, S.; Agmon, N. *J. Phys. Chem. A* **2009**, *113*, 6599–6606.
(46) Frisch, M. J.; et al. *Gaussian*, revision E.01; Gaussian, Inc.: Wallingford, CT, 2004.
(47) Vega, C. A.; Crespo, M. J. *J. Chem. Eng. Data* **1990**, *35*, 404–6.
(48) Mussini, P. R.; Mussini, T.; Rondinini, S. *Pure Appl. Chem.* **1997**, *69*, 1007–14.
(49) Krezel, A.; Bal, W. *J. Inorg. Biochem.* **2004**, *98*, 161–66.